Notes

Micro-Raman Spectroscopy as an in Situ Tool for Probing Radiation Damage during Microdiffraction Experiments in Soft Condensed Matter

Richard J. Davies,* Manfred Burghammer, and Christian Riekel

ESRF, 6 rue Jules Horowitz, BP220, 38043 Grenoble Cedex, France

Received July 1, 2008
Revised Manuscript Received July 19, 2008

Microfocus X-ray diffraction (micro-XRD) is a useful tool for studying the local structure of polymers and biopolymers.[1,2] It is also used routinely to study protein microcrystals.[3,4] One of the principal problems encountered with micro-XRD is radiation damage. This is particularly true for the high flux density submicrometer beams available at synchrotron radiation (SR) sources.[4] The impact of radiation damage depends upon the material being studied and the type of experiment being undertaken. While high-performance polymers may be resilient to radiation damage, hydrated β-starch becomes amorphous within a few seconds of irradiation.[5] Cryo-freezing organic or protein crystals can help reduce secondary radiation damage by immobilizing radicals produced by photoelectrons. This strategy is incompatible, however, with many types of in situ experiment.

Designing data collection strategies that can minimize radiation damage is becoming increasingly important, particularly as beam sizes decrease and SR sources become more brilliant. This requires a probe that can monitor radiation damage in situ and has a spatial resolution compatible with micrometer-scale X-ray beams. Near-edge X-ray absorption spectroscopy (NEXAFS/XANES) has been demonstrated as one approach for monitoring radiation damage in soft matter.[6,7] Its main disadvantage is its use of X-rays in both delivery and measurement capacities. Not only does this reduce its ability to monitor secondary radiation damage, it also precludes scanning experiments to measure the lateral extent of radiation damage from single exposures. Like NEXAFS, Raman spectroscopy has the capability to monitor specific molecular bonds within a material and can be used in a microfocus configuration. Unlike NEXAFS, its use of a low-powered laser as the excitation source allows data collection to be decoupled completely from X-ray induced radiation damage.

To demonstrate the potential of micro-Raman spectroscopy as a local probe for monitoring radiation damage, this study reports on the use of an in situ system to investigate localized radiation damage in a heterogeneous polypropylene (PP) specimen. The specimen is an isotactic polypropylene film containing regions of both α- and β-phase polypropylene (α and β). Scanning microdiffraction was carried out at the ID13 microfocus beamline of the ESRF. The beamline was configured for a wavelength of 0.1 nm from a channel-cut Si 111 monochromator. A pair of crossed Kirkpatrick−Baez (KB) mirrors provide a spot size at the focal position of 0.9 μm with a divergence of around 1 mrad. The flux was measured using a photodiode to be 2.1×10^{10} photons/s for a ring current of ~200 mA. This corresponds to a flux density of 1.3×10^8 photons/(s μm^2 mA). Diffraction patterns were collected using a 16-bit MAR165 CCD detector with a sample-to-film distance of 133.4 mm. For in situ Raman spectroscopy, a dedicated system was used, designed in collaboration with Renishaw PLC.[8] Simultaneous data collection is possible from the same sampling region by an on-axis focusing system. This delivers a 1.1 μm laser spot to the same position on the sample as the X-ray beam.[9]

For characterizing the PP specimen before and after X-ray exposure, 2D raster scans were performed. These covered an area of 200×200 μm^2, the extent of which is the region shown in Figure 1a. Characterization scans involved only micro-Raman data collection (5 μm step size, 5 s exposures). Between the two characterization scans an intermediate "irradiation" scan was performed with both X-ray and micro-Raman data collection (2.5 μm step size, 5 s exposures). This extended 100×100 μm^2, represented in Figure 1a as the inner square. It should be noted that all scans were carried out sequentially (in situ) without removing the sample. This ensured no change in focal spot or scan position between data collections.

Figure 1 shows parameter maps derived independently from the micro-Raman and micro-XRD data sets collected during the "irradiation" scan. This demonstrates simultaneous data collection from the same sampling region using both instruments. In Figure 1b, the position of the 808 cm^{-1} Raman band is plotted according to data collection position. This band is assigned to rocking and stretching vibrational modes of CH_2 and C−C bonds within helical chains in the crystalline region.[10] Figure 1c shows a complementary plot derived from the 210 β-phase reflection's integrated intensity, as determined from micro-XRD data. The correlation between the two plots reveals that the 808 cm^{-1} Raman band position is phase-sensitive. Such phase sensitivity provides a glimpse of how an in situ micro-Raman system can adopt the role of a sample alignment tool. This could reduce radiation damage by eliminating the need for alignment scans using X-rays.

Figures 2a,b show direct comparisons of Raman spectra corresponding to the α and β modifications collected before and after X-ray exposure. To eliminate the possibility of artifacts within individual spectra, each series represents an average over the same 10×10 μm^2 area. The approximate positions of these areas within the scan range are shown in Figure 1a, denoted by the numerals (i) and (ii). The results reveal that both of the polypropylene phases exhibit a reduction in Raman scattering intensity following X-ray exposure. This includes bands specific to both the crystalline and amorphous fractions, such as the 808 and 841 cm^{-1} bands.[10] There is also no significant increase in bands arising from nonhelical conformations, such as the 830 cm^{-1} Raman band observed in the polymer melt.[10] A similar comparison was also made for regions within the characterization scans that were not irradiated by the X-ray beam (i.e., outside the 100×100 μm^2 area shown in Figure 1a). These spectra did not show any change in intensity following X-ray exposure. This demonstrates that, although the differences in Figure 2 may be small, they can be attributed to irradiation with a high degree of certainty.

* Corresponding author. E-mail: rdavies@esrf.fr.

10.1021/ma801466j CCC: $40.75
Published on Web 08/30/2008

From the Raman spectrum of PP it is it possible to estimate crystallinity.[11,12] Nielsen et al. have shown that this approach provides values in good agreement with crystallinity data derived from differential scanning calorimetry (DSC) measurements.[10] The calculation is based upon the integrated intensities of a number of different Raman bands, as shown in the equation

$$x_c = \frac{I_{808\,\mathrm{cm}^{-1}}}{I_{808\,\mathrm{cm}^{-1}} + I_{830\,\mathrm{cm}^{-1}} + I_{841\,\mathrm{cm}^{-1}}} \quad (1)$$

Figures 3a,b show local variations in crystallinity over the 200 × 200 μm^2 scan region. Values were determined using eq 1 from data collected before and after X-ray exposure. Figure 3 reveals considerable point-to-point variations in local crystallinity within both data sets. The reduced variation observed in lateral spherulites can be attributed to partial polarization of the excitation source. Vibrations corresponding to the 808 and 841 cm^{-1} Raman bands contain a C−C stretch component and are therefore polarized parallel to the molecular helix.[13] Figure 3 shows no overall change in sample crystallinity as a result of X-ray exposure. This is confirmed by statistical analysis (a mean of 0.616 in both cases). By contrast, a difference is observed in total Raman scattering intensity, as shown in Figure 4. Data

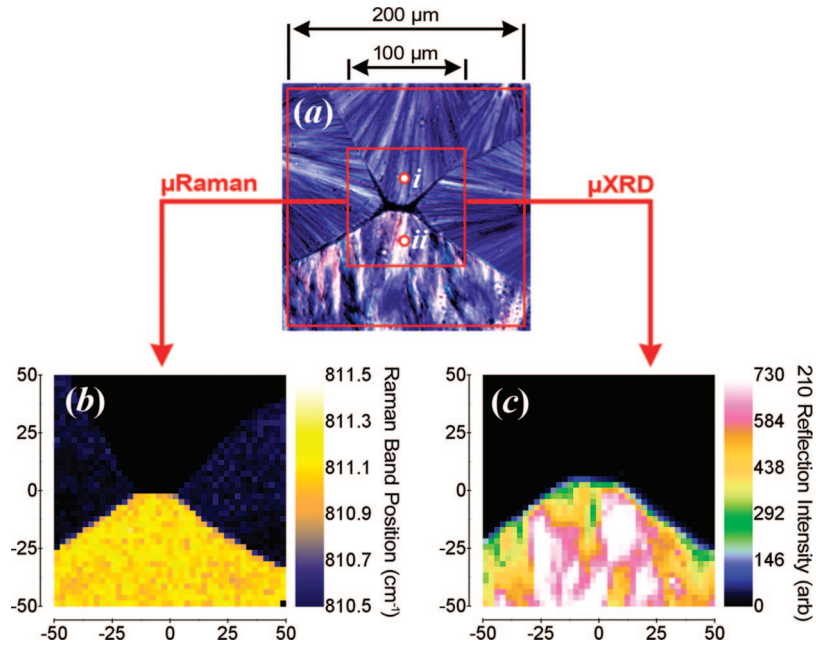

Figure 1. (a) Optical image of the specimen with scan ranges indicated. (b) Position of the 808 cm^{-1} Raman band and (c) the intensity of the 210 reflection. The two area maps, obtained simultaneously, reveal the spatial distribution of β-phase PP within the specimen.

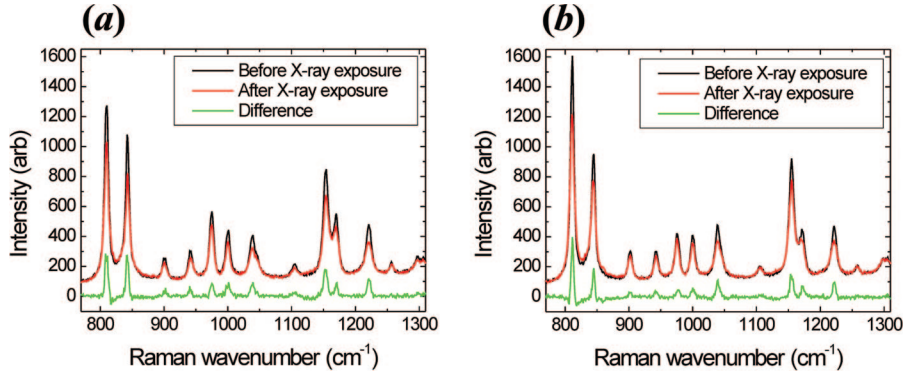

Figure 2. Micro-Raman spectra from (a) α-phase and (b) β-phase PP collected before and after X-ray irradiation. A difference series is also shown in each case.

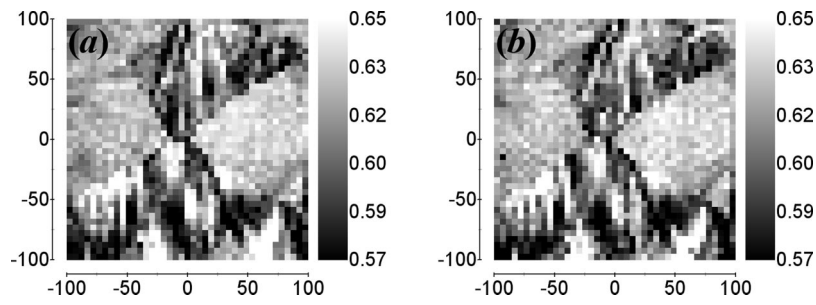

Figure 3. Variations in sample crystallinity derived from micro-Raman spectra collected (a) before and (b) after irradiation.

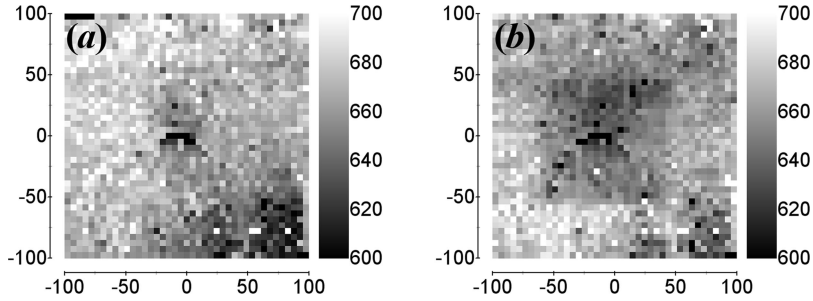

Figure 4. Variations in total integrated Raman scattering intensity (between 770 and 1310 cm^{-1}) collected (a) before and (b) after irradiation.

collected after X-ray exposure (Figure 4b) reveal a slightly darker area positioned at the center of the image. This feature is not seen in the first characterization scan, performed prior to irradiation (Figure 4a). Its location and size clearly match the micro-XRD scan region indicated in Figure 1a.

The results of this study suggest the degradation of PP during micro-XRD is dominated by mass loss associated with primary radiation damage. This involves molecular-scale fragmentation resulting from direct bond scission and is not phase specific. Secondary radiation damage in PP has been linked to accelerated degradation of the amorphous fraction, as studied by Gorelik et al. using γ-rays.[14] The lack of any crystallinity change in this study suggests free radial reactions are negligible. There is little existing information on X-ray beam damage in PP. However, the influence of electron beam exposure has been studied using IR spectroscopy. Kitching and Donald report mass loss in PP due to electron beam exposure, in addition to cross-linking and polymer oxidation.[15] There is no evidence of cross-linking between molecular chains due to carbon−hydrogen bond scission in this study and no obvious carbonaceous material (from optical assessment). An electron beam study by Wang et al. reports no change in crystallinity following irradiation, in support of the present results.[16] However, their observation of a radiation-induced conversion from the α to β modification was not observed.[16] Mass loss radiation damage mechanisms have also been reported for other polymer systems using NEXAFS.[17,18] This includes poly(methyl methacrylate) (PMMA) and poly(propylene oxide) (PPO).[17,18]

To conclude, the results of this study demonstrate the potential of combined micro-Raman and micro-XRD for investigating radiation damage in soft matter and provide a glimpse of future experimental possibilities which need not be limited to polymeric materials. The use of microcrystals has been suggested as a means to reduce secondary radiation damage by allowing the escape of photoelectrons from the irradiated volume.[19] Methods of obtaining quantitative information about radiation damage in biological crystals using electron density data are unreliable.[20] They are complicated by the loss of resolution during exposure,[6] suffer from model bias,[6] and require similar conformational changes in a substantial number of unit cells.[20] The use of combined micro-Raman and micro-XRD may overcome these limitations and permit radiation damage to be studied in much greater detail, allowing microcrystal scan strategies to be optimized.

Acknowledgment. The authors acknowledge financial support for the micro-Raman spectrometer through the EEC FP6 grant (SAXIER).

References and Notes

(1) Riekel, C.; Davies, R. J. *Curr. Opin. Colloid Interface Sci.* **2005**, *9*, 396–403.
(2) Riekel, C. *Rep. Prog. Phys.* **2000**, *63*, 233262.3.
(3) Riekel, C.; Burghammer, M.; Schertler, G. *Curr. Opin. Struct. Biol.* **2005**, *15*, 556–562.
(4) Schoeck, J.; Davies, R. J.; Martel, A.; Riekel, C. *Biomacromolecules* **2007**, *8*, 602–610.
(5) Lemke, H.; Burghammer, M.; Flot, D.; Roessle, M.; Riekel, C. *Biomacromolecules* **2004**, *5*, 1316–1324.
(6) Holton, J. M. *J. Synchrotron Radiat.* **2007**, *14*, 51–72.
(7) Hitchcock, A. P.; Dynes, J. J.; Johansson, G.; Wang, J.; Botton, G. *Micron* **2008**, *39*, 311–319.
(8) Davies, R. J.; Burghammer, M.; Riekel, C. *Appl. Phys. Lett.* **2005**, *87*, 264105.
(9) Davies, R. J.; Burghammer, M.; Riekel, C. *Macromolecules* **2006**, *39*, 4834–4840.
(10) Nielson, A. S.; Batchelder, D. N.; Pyrz, R. *Polymer* **2002**, *43*, 2671–2676.
(11) Gatos, K. G.; Minogianni, C.; Galiotis, C. *Macromolecules* **2007**, *40*, 786–789.
(12) Minogianni, C.; Gatos, K. G.; Galiotis, C. *Appl. Spectrosc.* **2005**, *59*, 1141–1147.
(13) Wang, X.; Michielsen, S. *J. Appl. Polym. Sci.* **2001**, *82*, 1330–1338.
(14) Gorelik, B. A.; Kolganova, I. V.; Matisov-i-Rychhi, L.; Listvojb, G. I.; Drabkina, A. M.; Golnik, A. G. *Polym. Degrad. Stab.* **1993**, *42*, 263–266.
(15) Kitching, S.; Donald, A. M. *J. Microsc.* **1998**, *190*, 357–365.
(16) Wang, G. H.; Li, X. Y.; Lu, Y. Y.; Zhu, Y. Z.; Wang, H. W.; Dou, L.; Yu, R. X. *Z. Phys. B: Condens. Matter* **1987**, *65*, 347–351.
(17) Coffey, T.; Urquhart, S. G.; Ade, H. *J. Electron Spectrosc. Relat. Phenom.* **2002**, *122*, 65–78.
(18) Beetz, T.; Jacobsen, C. *J. Synchrotron Radiat.* **2002**, *10*, 280–283.
(19) Nave, C.; Hill, M. A. *J. Synchotron Radiat.* **2005**, *12*, 299–303.
(20) Kmetko, J.; Husseini, N. S.; Naides, M.; Kalinin, Y.; Thorne, R. E. *Acta Crystallogr.* **2006**, *D62*, 1030–1038.

MA801466J